

Effect of ganglioside GT1b on the *in vitro* maturation of porcine oocytes and embryonic development

Seon-Ung HWANG¹, Yubyeol JEON¹, Junchul David YOON¹, Lian CAI¹, Eunhye KIM¹, Hyunju YOO¹, Kyu-Jun KIM¹, Kyu Mi PARK¹, Minghui JIN¹, Hyunggee KIM² and Sang-Hwan HYUN¹

¹Laboratory of Veterinary Embryology and Biotechnology, College of Veterinary Medicine, Chungbuk National University, Chungbuk 362-763, South Korea

²Department of Biotechnology, School of Life Sciences and Biotechnology, Korea University, Seoul 136-713, South Korea

Abstract. Ganglioside is an acidic glycosphingolipid with sialic acids residues. This study was performed to investigate the effect and mechanism of ganglioside GT1b in porcine oocytes in the process of *in vitro* maturation (IVM) and preimplantation development. Metaphase II (MII) rates were significantly ($P < 0.05$) different between the control group and the 5 nM GT1b treatment group. Intracellular glutathione (GSH) levels in oocytes matured with 5 nM and 20 nM and GT1b decreased significantly ($P < 0.05$). The 10 nM group showed a significant ($P < 0.05$) decrease in intracellular reactive oxygen species (ROS) levels compared with the control group. Subsequently, the level of intracellular Ca^{2+} in oocytes treated with different concentrations of GT1b was measured. Intracellular Ca^{2+} was significantly ($P < 0.05$) increased with a higher concentration of GT1b in a dose-dependent manner. Real-time PCR was performed and showed that the expression of *bradykinin 2 receptor (B2R)* and *calcium/calmodulin-dependent protein kinase II delta (CaMKII δ)* in cumulus cells was significantly ($P < 0.05$) decreased in the 20 nM GT1b treatment group. Treatment with 5 nM GT1b significantly ($P < 0.05$) decreased the expression of *CaMKII δ* . In oocytes, treatment with 5 nM GT1b significantly ($P < 0.05$) decreased *CaMKII γ* and *POU5F1 (POU domain, class 5, transcription factor 1)*. However, treatment with 20 nM GT1b significantly ($P < 0.05$) increased the expression of *POU5F1*. Finally, embryonic developmental data showed no significant differences in the two experiments (parthenogenesis and *in vitro* fertilization). In conclusion, the results of the present study indicated that GT1b plays an important role in increasing the nuclear maturation rate and decreasing the intracellular ROS levels during IVM. However, GT1b inhibited maturation of the cytoplasm by maintaining intracellular Ca^{2+} in the process of oocyte maturation regardless of the cell cycle stage. Therefore, GT1b is thought to act on another mechanism that controls intracellular Ca^{2+} .

Key words: Embryonic development, Ganglioside GT1b, Intracellular calcium, *In vitro* maturation (IVM), Porcine (J. Reprod. Dev. 61: 549–557, 2015)

Pigs are anatomically and physiologically similar to humans, and in the field of regenerative medicine, it is known that is suitable in comparison with mice and rats. However, the *in vitro* maturation system for pig oocytes is still inefficient, mainly due to the loss of the developmental capacity in the preimplantation stage [1]. This inefficiency might be associated with an insufficient understanding of the epigenetic mechanisms of porcine oocytes during *in vitro* maturation (IVM), macro- and micronutrients, endocrine status and oxidative stress compared with our understanding of other mammals [2, 3].

To date, porcine IVM conditions have been improved by treatment with various antioxidants, such as melatonin [4–6] and resveratrol

[7–9], and growth factors, such as epidermal growth factor (EGF) [10–12], granulocyte-macrophage colony-stimulating factor (GM-CSF) [13] and vascular endothelial growth factor (VEGF) [14, 15]. Through these studies, the quality of porcine oocytes has shown some improvement. In a recent study, it was also confirmed that a glycosphingolipid called ganglioside is diversely expressed in the process of mouse embryonic development [16].

Ganglioside is an acidic glycosphingolipid that has sialic acids residues and is known to play an important role in biological processes, such as cell differentiation, adhesion, regulation of growth and signal transduction [17]. Specifically, it is distributed mainly in the central nervous system and is involved in the development of the brain and memory [18, 19]. The structure of gangliosides includes a sugar chain with one or more sialic acid (e.g., n-acetylneuraminic acid, NANA) residue. More than 60 gangliosides exist according to the number and the position of the NANA residues. They can be classified into a-, b- and c-series gangliosides according to the number of sialic acids bound to the galactose portion of the molecule [20]. The a-series includes GM3, GM2, GM1, GD1a and GT1a; the b-series includes GD3, GD2, GD1b, GT1b and GQ1b; and the c-series includes GT3, GT2, GT1c, GQ1c, and GP1c [21].

Received: May 7, 2015

Accepted: August 6, 2015

Published online in J-STAGE: September 12, 2015

©2015 by the Society for Reproduction and Development

Correspondence: HG Kim (e-mail: hg-kim@korea.ac.kr) and SH Hyun (e-mail: shhyun@cbu.ac.kr)

This is an open-access article distributed under the terms of the Creative Commons Attribution Non-Commercial No Derivatives (by-nc-nd) License <<http://creativecommons.org/licenses/by-nc-nd/3.0/>>.

In the mouse, the role of ganglioside in early embryonic development has been investigated. One of the b-series gangliosides GT1b was reported to suppress mitochondrial DNA (mtDNA) damage resulting from ROS in the mouse brain [22]. Moreover, it was shown that GT1b decreases DNA fragmentation and apoptotic changes by reducing ROS by blocking the diffusion of H₂O₂ into the sperm membrane in humans [23, 24]. GT1b expression was observed during the embryonic developmental process of mice using cryopreservation and a thawing method at different developmental stages [25]. It was also observed that the addition of GT1b into the culture media for rat hippocampal cells or neuroblastoma–glioma hybridoma (NG108-15) cells temporarily activated CaMKII [26]. In addition, it was recently reported that the B2R is part of the signal transduction pathway that is related to the maturation and differentiation of neurons induced by GT1b B2R activated by binding with Gq/11, which results in activation of phospholipase C (PLC), resulting in the production of inositol triphosphate (IP3) and diacylglycerol (DAG). IP3 is able to induce Ca²⁺ release from the endoplasmic reticulum, and DAG stimulates protein kinase (PK) C [27]. Increased Ca²⁺ in the cumulus cells during this process is thought to diffuse into the egg through the gap junction, which would cause activation of CaMKII and likely to play an important role in the maturation of oocytes (Fig. 2) [28].

However, GT1b is thought to contribute to the maturation of oocytes and the survival of embryonic development. So far, a number of studies have been conducted to identify the physiological functions and biological activities of GT1b in rodents; however, limited information is available regarding the effects of GT1b on the maturation of porcine oocytes. In the present study, the effect of GT1b treatment on porcine oocyte maturation and the subsequent preimplantation embryonic development was investigated.

Materials and Methods

Chemicals

Trisialoganglioside GT1b (NH₄⁺ salt) (Matreya LLC, 1063) was dissolved in deionized (DI) water to make a 1 mM stock solution. Stock solutions were stored at –20 C until required, at which time they were added to the oocyte maturation medium in specific amounts according to the experimental protocol. All of the other chemicals were purchased from Sigma-Aldrich Chemical Company (St. Louis, MO, USA).

Oocyte collection and IVM

Porcine ovaries were collected from a slaughterhouse. Porcine follicular fluid (pFF) and cumulus–oocyte complexes (COCs) were recovered from 3–6 mm ovarian follicles using an aspiration method. The medium used during IVM was composed of TCM199 (Gibco, Life Technologies, Melbourne, Australia), 0.6 mM cysteine, 0.91 mM sodium pyruvate, 10 ng/ml epidermal growth factor, 75 µg/ml kanamycin, 1 µg/ml insulin, 10% (v/v) and pFF. GT1b was used to treat the oocytes during IVM at concentrations of 0 µM, 5 µM, 10 µM and 20 µM. Porcine COCs were co-cultured at 50 to 60 cells per well using a 4-well dish (Nunc, Roskilde, Denmark) with 500 µl of IVM medium (0 µM group). 20 µl of DI water was added to all groups. IVM was performed at 39 C in 5% CO₂ using a humid incubator (Astec, Fukuoka, Japan). Maturation was performed in

IVM media with 10 IU/ml equine chorionic gonadotropin (eCG) and 10 IU/ml human chorionic gonadotropin (hCG) for 22 h. The cells were then moved into hormone-free IVM medium and cultured for 18 h. Matured COCs were denuded by gentle pipetting with 0.1% hyaluronidase and TLH-PVS medium. Cumulus cells and denuded oocytes were obtained through this process and then used for subsequent experiments.

Assessment of nuclear maturation

Nuclear maturation of denuded oocytes was evaluated using 10 µg/ml Hoechst 33342 dye. Fluorescence was observed under an inverted fluorescence microscope (TE300, Nikon, Tokyo, Japan) with UV filters (330–385 nm) at 400 × magnification. Nuclear maturity was assessed by classifying cells into four stages (germinal vesicle, metaphase I, anaphase and telophase I and metaphase II).

Measurement of intracellular GSH and ROS levels

The intracellular GSH and ROS levels in matured oocytes were measured using 4-chloromethyl-6,8-difluoro-7-hydroxycoumarin (CellTracker Blue CMF2HC, Invitrogen, Carlsbad, CA, USA) and 2',7'-dichlorodihydrofluorescein diacetate (DCF-DA, Invitrogen), respectively. Details of the protocol were described previously [7, 29, 30]. In short, the matured oocytes were added to 10 µM H2DCFDA or 10 µM CellTracker Blue with TLH-PVA medium and stained for 30 min in the dark. The stained oocytes were washed with TLH-PVA medium, and then, 10 oocytes were transferred to one drop of TLH-PVA medium. Fluorescence was observed under an inverted fluorescence microscope with UV filters (460 nm for ROS and 370 nm for GSH) at 200 × magnification. Fluorescent images were saved as picture files in jpeg format. Using the Adobe Photoshop software (version 13.0, Adobe Systems, San Jose, CA, USA), fluorescence intensity was measured only in the cytoplasmic portion of the oocytes.

Parthenogenetic activation (PA) and in vitro culture (IVC)

Oocytes at the stage of metaphase II were chosen for PA, and they were activated with two pulses of 120 V/mm DC for 60 µsec in a 260 mM mannitol solution containing 0.1 mM CaCl₂ and 0.05 mM MgCl₂. After electrical activation, the PA embryos were incubated in 5 µg/ml cytochalasin B (CB) in drops of porcine zygote medium (PZM) for 4 h. Embryos were transferred to a PZM drop for IVC. On the second day after activation, embryo cleavage was evaluated (1 cell, 2 cell, 4 cell, 8 cell, fragment) and transferred to a new PZM drop. On the 7th day after activation, blastocyst (BL) formation was evaluated quantitatively (early BL, expanded BL, hatched BL) and qualitatively (total cell number per BL) using 10 µg/ml Hoechst 33342.

In vitro fertilization (IVF)

Among denuded oocytes, MII-stage, oocytes were selected and washed two times using mTBM, and 15 oocytes were then transferred to an mTBM drop. The motility and concentration of sperm in liquid semen was confirmed using a hemocytometer. The final concentration of sperm was diluted to 5 × 10⁵/ml and co-cultured with oocytes at 39 C in a 5% CO₂ humid incubator for 20 min. Next, sperm on the surface of oocytes were detached by gentle pipetting and moved

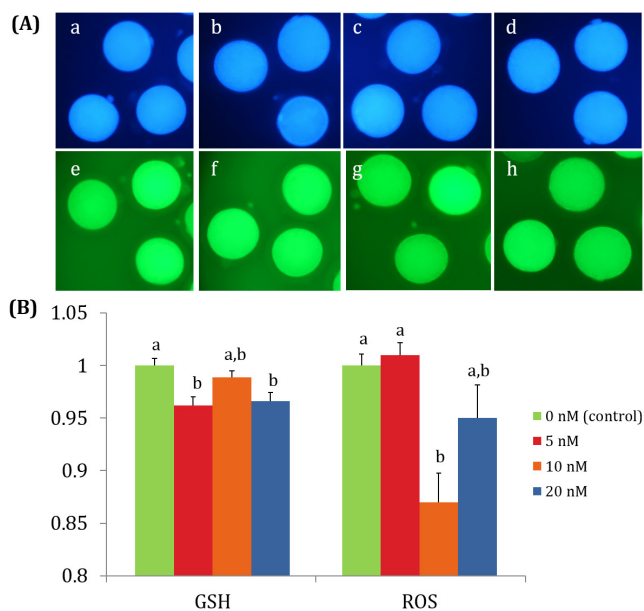


Fig. 1. Measurement of intracellular glutathione (GSH) and reactive oxygen species (ROS) levels in matured oocytes. (A) Fluorescent photomicrographic images of *in vitro* matured porcine oocytes. Oocytes were stained with CellTracker Blue (a–d) and 2',7'-dichlorodihydrofluorescein diacetate (DCF-DA) (e–h). Metaphase II (MII) oocytes derived from the maturation medium supplemented 0 μ M (a and e), 5 μ M (b and f), 10 μ M (c and g) and 20 μ M GT1b (d and h). (B) Effect of the ganglioside GT1b in the maturation medium on intracellular GSH and ROS levels in *in vitro* matured porcine oocytes. Within each group (GSH and ROS) at the end point, bars with different letters (a–b) are significantly ($P < 0.05$) different. GSH samples, $N = 50$; ROS samples, $N = 65$. Experiments were replicated three times.

to an mTBM drop. Embryos were cultured at 39 C in a 5% CO₂ humid incubator for 5 h. They were then transferred to PZM drops for IVC, and embryonic development was evaluated using the same method as used for PA.

Reverse transcription and quantitative real-time PCR

TRizol reagent (Invitrogen) was used to extract total RNA from matured cumulus cells. To synthesize cDNA from the extracted total RNA, Moloney murine leukemia virus (MMLV) reverse transcriptase and random primers (Invitrogen) were used. All procedures were carried out according to the manufacturer's instructions. A SuperPrep™ Cell Lysis & RT Kit for qPCR (Toyobo, Osaka, Japan) was used for total RNA extraction and the synthesis of cDNA in matured oocytes according to the manufacturer's instructions. Quantitative real-time PCR (Mx3000P qPCR, Agilent Technologies, Santa Clara, CA, USA) analysis was conducted using the synthesized cDNA and 2 \times SYBR Premix Ex Taq (Takara Bio, Otsu, Shiga, Japan). All of the primer sequences are presented in Table 1. The reactions were performed for 40 cycles, and the cycling parameters were as follows: denaturation at 95 C for 30 sec, annealing at 57 C for 30 sec, and extension at 72 C for 30 sec. Relative quantification was based on a comparison of the threshold cycle (Ct) at constant fluorescence intensity. The

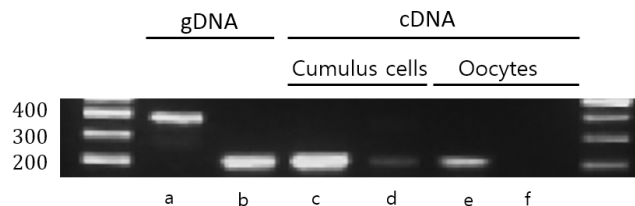


Fig. 2. Identification of B2R gene expression in matured cumulus cells and oocytes. Genomic DNA (gDNA) and complementary DNA (cDNA) polymerase chain reaction analysis of *GAPDH* (gDNA, 374 bp and cDNA, 207 bp) and B2R (gDNA and cDNA, 196 bp). a, c and e: *GAPDH*. b, d and f: *B2R*. *GAPDH* was used a control.

relative mRNA expression (R) was calculated using the equation $R = 2^{-[\Delta C_t \text{ sample} - \Delta C_t \text{ control}]}$. To determine a normalized arbitrary value for each gene, every value was normalized to that of *GAPDH* [31].

Intracellular Ca²⁺ staining

The denuded oocytes were stained using TCM199 with 5 μ M Fluo-4, AM, at 39 C in a 5% CO₂ humid incubator for 40 min. Next, oocyte nuclei were stained using TLH-PVA solution with 10 μ g/ml Hoechst 33342 dye for 5 min. Stained oocytes were washed with TLH-PVA solution and placed in a confocal dish (Invitrogen) before being covered with a cover glass to immobilize them. Next, the distribution of intracellular Ca²⁺ in the oocytes was investigated using confocal laser microscopy (Carl Zeiss, Thornwood, NY, USA). All of the images were analyzed with the ZEN 2009 Light Edition software.

Statistical analysis

All of the experiments were replicated more than three times. All data were analyzed by one-way ANOVA followed by Duncan's test using SPSS (Statistical Package for the Social Sciences) and are reported as the mean \pm SEM. Differences were considered to be significant if the P-value was less than 0.05.

Results

Enhancement of nuclear maturation on oocytes by GT1b

The nuclear maturation of oocytes at each stage, germinal vesicle (GV), metaphase I (MI), anaphase and telophase I (Ana & Telo I) and metaphase II (MII), was evaluated after IVM for 40 h. The experiment was repeated 4 times. The results showed that the percentages of immature stage cells in the treated groups, including cells at the GV, MI and Ana & Telo I stages, were not significantly ($P < 0.05$) different compared with the control (GV, MI and Ana & Telo I stages: 2.0, 6.6 and 12.5% for the control; 0.6, 6.4 and 6.4% for the 5 nM GT1b group; 0.6, 5.1 and 11.4% for the 10 nM GT1b group; and 1.3, 10 and 8.8% for the 20 nM GT1b group, respectively). The rate of matured MII-stage cells after treatment with 5 nM GT1b was 86.6%, which was significantly ($P < 0.05$) higher than that of the control group (78.9%). However, the other treatment (82.9 and 80.0% for the 10 nM and 20 nM GT1b groups, respectively) did not show a significant ($P < 0.05$) differences compared with the control (Table 2).

Table 1. Primer sequences for analysis of mRNA gene expression

mRNA	Primer sequences	Tm	Product size (bp)	GenBank accession number
<i>GAPDH</i>	F: 5'-GTCGGTTGTGGATCTGACCT-3'	60.5	207	NM_001206359
	R: 5'-TTGACGAAAGTGGTCGTTGAG-3'	58.4		
<i>PCNA</i>	F: 5'-CCTGTGCAAAAAGATGGAGTG-3'	57.3	187	XM_003359883
	R: 5'-GGAGAGAGTGGAGTGGCTTT-3'	59.8		
<i>POU5F1 (Oct4)</i>	F: 5'-GCGGACAAGTATCGAGAACC-3'	59.3	200	NM_001113060
	R: 5'-CCTCAAAATCCTCTCGTTGC-3'	57.3		
<i>Bax</i>	F: 5'-TGCCTCAGGATGCATCTACC-3'	59.3	199	XM_003127290
	R: 5'-AAGTAGAAAAGCGCACCAC-3'	57.3		
<i>Bcl-2</i>	F: 5'-AATGACCACCTAGAGCCTTG-3'	58.4	182	NM_214285
	R: 5'-GGTCATTTCCGACTGAAGAG-3'	58.4		
<i>Caspase-3</i>	F: 5'-CGTGCTTCTAAGCCATGGTG-3'	59.3	186	NM_214131
	R: 5'-GTCCCACTGTCCGTCTCAAT-3'	59.3		
<i>B2R</i>	F: 5'-GCTCTACAGCCTGGTGATCT-3'	57.1	206	NM_214146
	R: 5'-TGCAGTAGGTGATGATGCTC-3'	57.3		
<i>CaMKIIδ</i>	F: 5'-ACAGTACCCATCAAGCCATC-3'	57.5	199	NM_214381
	R: 5'-ATGCATGAAGAGGAGGAGAG-3'	57.0		
<i>CaMKIIγ</i>	F: 5'-CTTATCCAAGAACAGCAAGC-3'	55.3	202	NM_214193
	R: 5'-GCAGTGGTAGTGGACATTGA-3'	57.1		

F: forward, R: reverse.

Table 2. Effect of GT1b treatment on nuclear maturation during IVM

GT1b concentration (nM)	Oocytes cultured for maturation, N*	Number of oocytes at the stage of			
		Germinal vesicle (%)	Metaphase I (%)	Anaphase and telophase I (%)	Metaphase II (%)
0	152	3 (2.0 ± 0.7)	10 (6.6 ± 1.5)	19 (12.5 ± 2.0)	120 (78.9 ± 1.3) ^a
5	157	1 (0.6 ± 0.7)	10 (6.4 ± 2.0)	10 (6.4 ± 1.5)	136 (86.6 ± 1.1) ^b
10	158	1 (0.6 ± 0.5)	8 (5.1 ± 1.3)	18 (11.4 ± 1.3)	131 (82.9 ± 0.7) ^{a,b}
20	160	2 (1.3 ± 0.7)	16 (10.0 ± 4.4)	14 (8.8 ± 2.9)	128 (80.0 ± 2.5) ^{a,b}

Values with different superscript letters (a, b) within a column differ significantly ($P < 0.05$). The data represent the means ± SEM. * The experiment was replicated four times.

GSH and ROS levels were decreased by GT1b

MII-stage oocytes were selected after IVM for 40 h, and GSH and ROS were measured. The GSH levels in the 5 nM and 20 nM treatment groups were significantly lower than that of the control group. The 10 nM treatment group did not show a significant difference compared with the control. The ROS level in the 10 nM treatment group was significantly lower than that in the control group. The other treatment groups (5 nM and 20 nM treatment groups) did not demonstrate a significant differences compared with the control group (Fig. 1).

Expression of B2R was observed in cumulus cells but not in oocytes

B2R expression was confirmed by reverse transcription PCR. According to a previous study, bradykinin 2 is known to activate CaMKII in response to GT1b stimulation [32]. The PCR results revealed the B2R gene (gDNA and cDNA, 196 bp) in the porcine genomic DNA (gDNA). Expression of B2R mRNA was observed

in cDNA of cumulus cells but not in oocytes. Expression of the GAPDH gene (gDNA, 374 bp and cDNA, 207 bp) was used as a control in all groups (Fig. 2).

Matured cumulus cells and oocytes showed completely different patterns of mRNA expression

To analyze the mechanism of effect of GT1b on IVM, we examined the expression of apoptosis-associated genes (*Bax*, *Bcl-2*, *Caspase-3*) and *PCNA*, *POU5F1*, *B2R* and CaMKII subunit genes (*CaMKII γ* and *CaMKII δ*) in matured cumulus cells and oocytes. In cumulus cells, the 20 nM treatment group showed significantly ($P < 0.05$) decreased the expression of B2R. The expression of *CaMKII δ* was significantly decreased in all treatment groups ($P < 0.05$) (Fig. 3A). In oocytes, the expression of *POU5F1* was significantly decreased in the 5 nM treatment group ($P < 0.05$), whereas its expression was significantly increased in the 20 nM treatment group ($P < 0.05$). The 5 nM treatment group exhibited significantly ($P < 0.05$) increased expression of *CaMKII γ* (Fig. 3B).

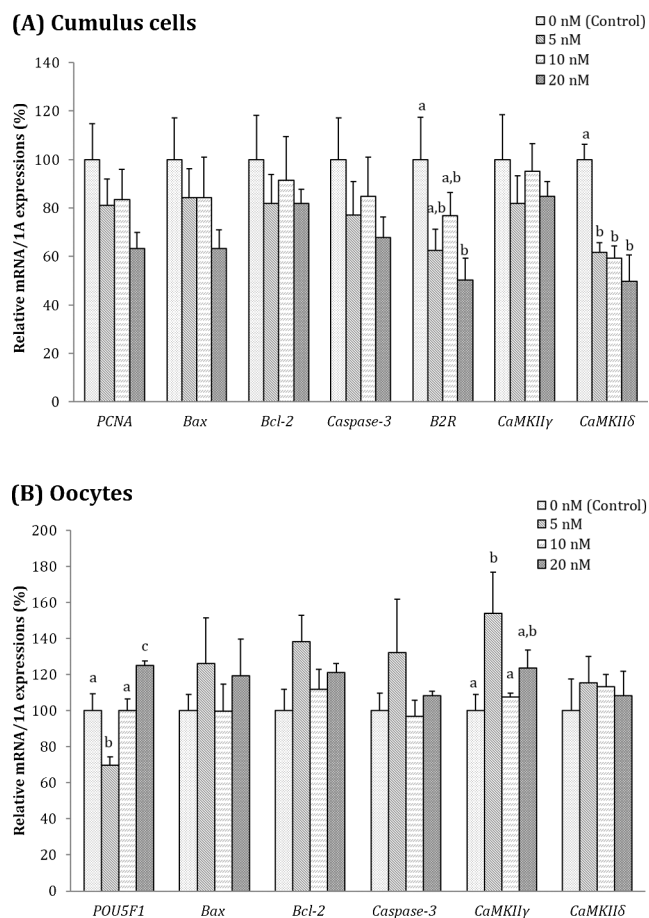


Fig. 3. Expression levels of genes relative to apoptosis and calcium signaling were determined by quantitative RT-PCR. Mean \pm SEM expression of proliferating cell nuclear antigen (*PCNA*), pluripotency-associated gene (*POU5F1*), apoptosis-associated genes (*Bax*, *Bcl-2*, *Caspase-3*), bradykinin 2 receptor (*B2R*) and Ca^{2+} /calmodulin-dependent protein kinase type II subunit (*CaMKII γ* and *CaMKII δ*) mRNA in matured (A) cumulus cells and (B) oocytes treated with the ganglioside GT1b during *in vitro* maturation (IVM). Within the same mRNA, values with different superscript letters differ significantly ($P < 0.05$). The experiment was replicated three times.

The intracellular Ca^{2+} concentration was maintained irrespective of the cell cycle in oocytes in the GT1b treatment groups

Oocytes were classified by stage using Hoechst staining to confirm the distribution of Ca^{2+} according to the degree of nuclear maturation, and intracellular Ca^{2+} in oocytes was stained using Fluo-4, AM, and observed based on the fluorescence intensity. The results showed that the intracellular Ca^{2+} level was significantly increased from the GV stage (16.41 ± 0.31) to the GVBD stage (29.30 ± 0.23), but oocytes in the MI stage (31.88 ± 3.94) did not show a significant ($P < 0.05$) difference. However, in the MII stage (10.48 ± 2.10), the intracellular Ca^{2+} level was significantly decreased in the MII stage (10.48 ± 2.10) and reached the level of the GV stage ($P < 0.05$) (Fig. 4).

Next, the intracellular Ca^{2+} level was evaluated in oocytes at 18 h and 40 h after IVM initiation, which are thought to be mainly

in the MI stage, to identify the change in intracellular Ca^{2+} level in oocytes after GT1b treatment [33]. The results showed that the fluorescence intensity of cells that underwent 18 h of IVM and were treated with 5 nM GT1b was significantly decreased compared with the control and that other groups did not show a significant differences ($P < 0.05$). However, the Ca^{2+} fluorescence intensity of cells that underwent 40 h of IVM and were treated with 5 nM GT1b was significantly ($P < 0.05$) increased compared with the control. The Ca^{2+} fluorescence intensity of cells treated with 20 nM GT1b was significantly increased compared with that of the cells in the 5 nM treatment group (Fig. 5).

GT1b tended to improve development of preimplantation embryo

The cleavage and blastocyst formation rates of parthenogenetic embryo were evaluated 2 days and 7 days after the electrical activation. There were no significant differences between the control group and treatment groups. However, there was a tendency for a dose-dependent increase in both cleavage ratio and blastocyst development rate. Furthermore, the blastocyst formation rate was significantly different between the 5 nM and 20 nM treatment groups (Fig. 6).

The cleavage and blastocyst formation rates of fertilized embryo were evaluated 2 days and 7 days after fertilization. There were no significant differences between the control group and treatment groups (Fig. 7).

Discussion

Ganglioside is abundant in the nervous system and is thought to play an important role [18, 19]. However, in a recent study using a mouse model, it was confirmed that various types of gangliosides are dynamically expressed during embryonic development [25]. Gangliosides can be classified by the number of sialic acid residues. Among them, the b-series ganglioside GT1b is thought to stimulate B2R during neuronal differentiation in mice, which results in changes in the Ca^{2+} concentration [26]. In addition, some studies using mouse and human germ cells revealed that GT1b reduced ROS and DNA damage [22–25, 34]. Therefore, this study was performed to examine the effect of ganglioside on porcine germ cells.

GT1b forms micelles when it is dissolved in an aqueous solution [35]. Attachment of these micelles to the cell surface increases the diffusion barrier [36]. Micelles of GT1b also reduce mtDNA damage by an antioxidant effect in neurons. [22, 34] and protect spermatozoa from hydrogen peroxidase-induced DNA and membrane damage [23].

In the present study, we first evaluated the effect of GT1b on oocyte maturation by examining, nuclear maturation and cytoplasmic maturation were examined. Although the nuclear maturation rate of MII-stage oocytes in the 5 nM treatment group was significantly increased compared with that of the control, the GSH levels in the 5 nM and 20 nM treatment groups were lower than that in the control group. Interestingly, the ROS level in the 10 nM treatment group was significantly lower than those in the control and 5 nM treatment groups. In previous reports of porcine IVM, various antioxidants, including resveratrol [7–9], cysteine [34] and β -mercaptoethanol [37], increased intracellular GSH levels and reduced ROS levels in matured oocytes. These antioxidants showed positive effects

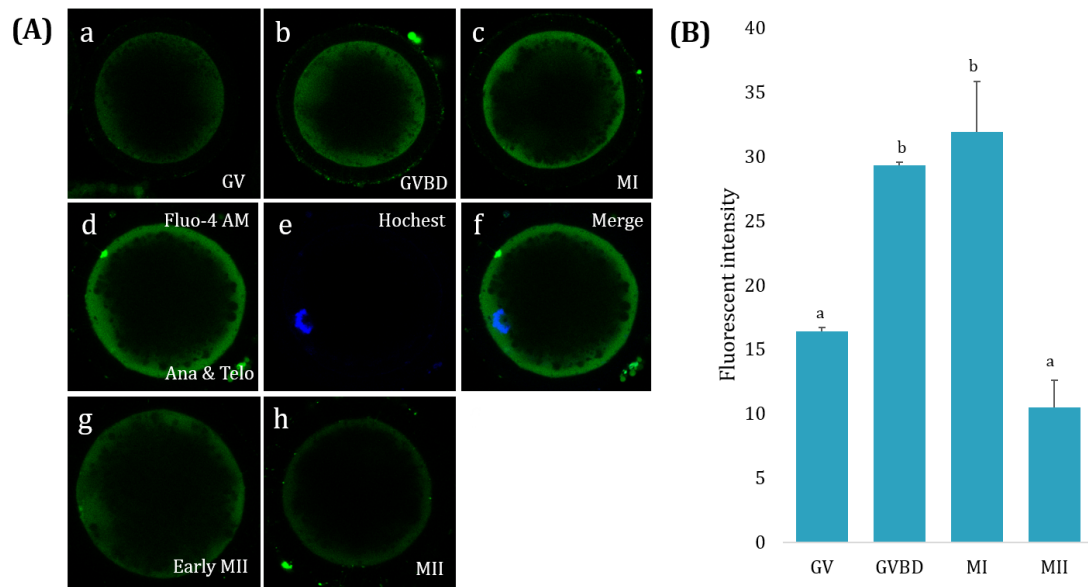


Fig. 4. Measurements of the Ca²⁺ concentration in oocytes according to the cell cycle. (A) Ca²⁺ distribution in porcine oocytes during different phases of *in vitro* maturation. a) Germinal vesicle (GV) stage, b) germinal vesicle breakdown (GVBD) stage, c) MI stage, d–f) anaphase & telophase stage, g) early MII stage, h) MII stage. (B) Comparison of Ca²⁺ fluorescence intensity in matured porcine oocytes treated with the ganglioside GT1b during *in vitro* maturation (IVM). Within each end point, bars with different letters (a, b) are significantly ($P < 0.05$) different for different concentrations of GT1b treatment.

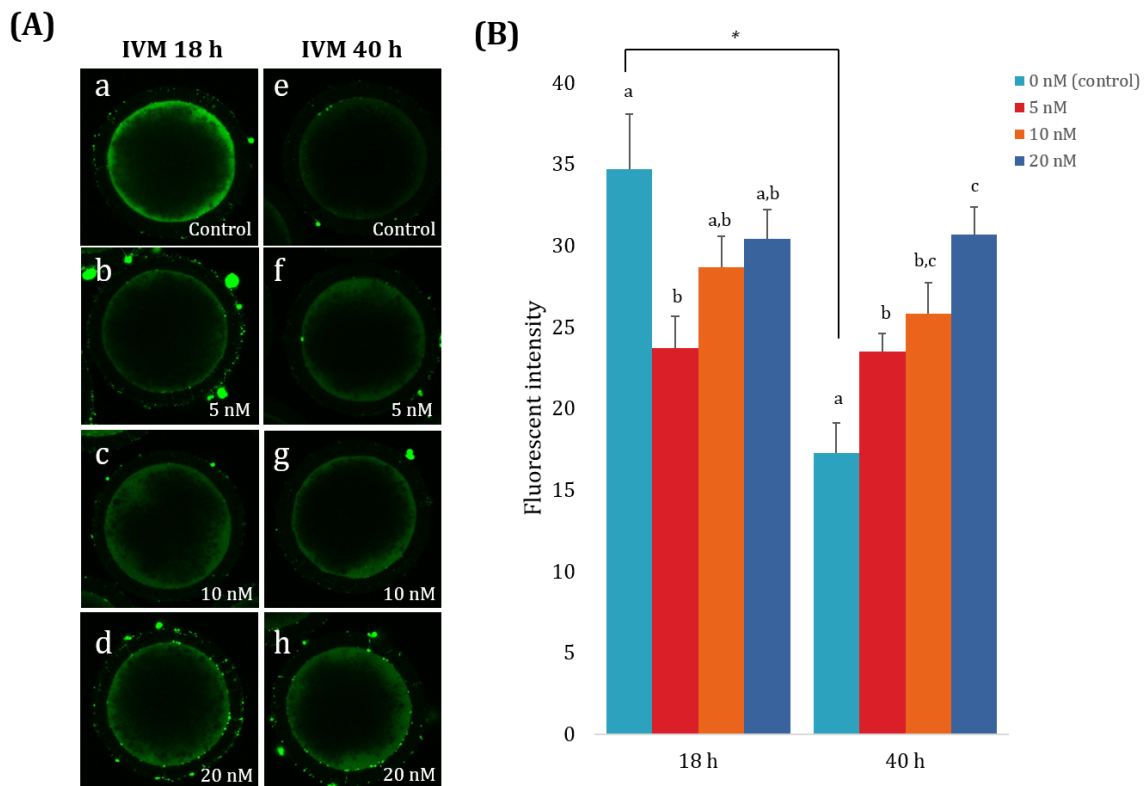


Fig. 5. Measurements of the Ca²⁺ concentration in matured porcine oocytes treated with the ganglioside GT1b during *in vitro* maturation (IVM). (A) Ca²⁺ distribution in matured porcine oocytes treated with the ganglioside GT1b. (a and e) 0 nM (control), (b and f) 5 nM, (c and g) 10 nM, (d and h) 20 nM. (B) Comparison of Ca²⁺ fluorescence intensity in matured porcine oocytes treated with the ganglioside GT1b. Within each end point, bars with different letters (a, b, c) are significantly ($P < 0.05$) different for different concentrations of GT1b treatment. * $P < 0.05$.

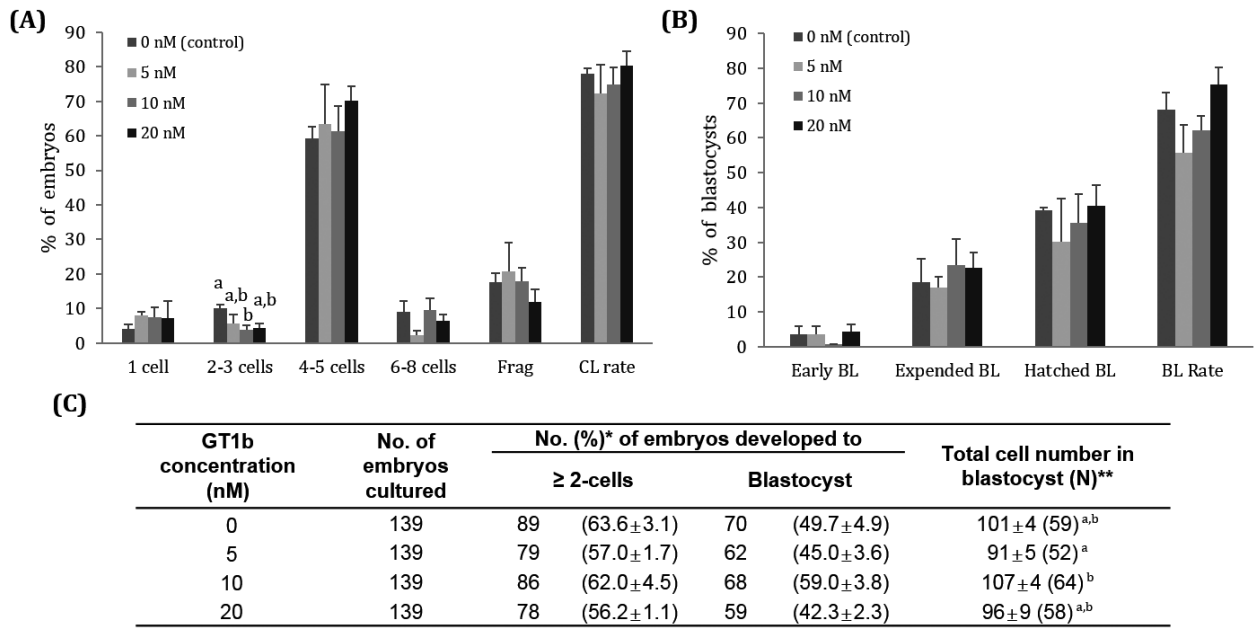


Fig. 6. Effect of GT1b treatment during IVM on embryonic development after parthenogenetic activation (PA) in terms of (A) the cleavage pattern and (B) the blastocyst formation pattern of the PA embryo. Within each end point, bars with different letters (a, b) are significantly ($P < 0.05$) different for different concentrations of GT1b treatment. CL, cleavage; BL, blastocyst. (C) Summary of embryonic development after PA. The cleavage rate was measured on day 2, and the blastocyst formation rate was evaluated on day 7 of culture.

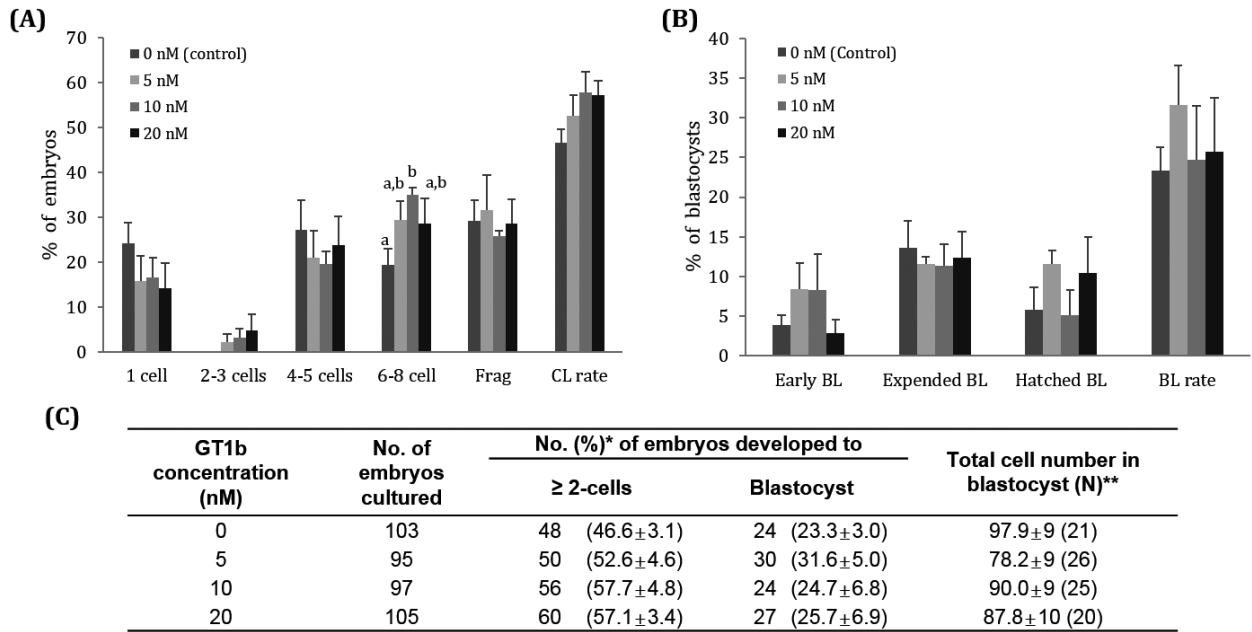


Fig. 7. Effect of GT1b treatment during IVM on embryonic development after *in vitro* fertilization (IVF) in terms of (A) the cleavage pattern and (B) the blastocyst formation pattern of IVF embryo. Within each end point, bars with different letters (a, b) are significantly ($P < 0.05$) different for different concentrations of GT1b treatment. CL, cleavage; BL, blastocyst. (C) Summary of embryonic development after IVF. The cleavage rate was measured on day 2, and the blastocyst formation rate was evaluated on day 7 of culture.

on oocyte maturation and embryonic development by improving cytoplasmic maturation. ROS are generated in the form of superoxide radicals, hydrogen peroxide and hydroxyl radicals as a necessity in the process of aerobic respiration to produce energy in cells [38–41]. Due to their high reactivity, they are thought to trigger cell damage due to cell membrane degeneration, protein degeneration, lipid oxidation, DNA damage and the inhibition of DNA synthesis [42, 43]. Oxidative stress due to ROS formation can be suppressed by endogenous antioxidant enzymes, such as superoxide dismutase, catalase, and glutathione peroxidase [44, 45]. However, the partial pressure of oxygen *in vitro* is higher than that *in vivo*, leading to the accumulation of ROS, which in turn generates oxidative stress. Oxidative stress *in vitro* causes a lower maturation rate during IVM and a lower embryonic development rate [46–49]. In this study, treatment with 10 nM GT1b did not result in a significant difference in GSH antioxidant expression compared with the control. However, 5 nM and 10 nM of GT1b result in rather lower expression of GSH. Therefore, other antioxidative mechanisms, but not GSH, might help reduce ROS during porcine IVM.

As one of the ROS reduction mechanisms, the intracellular Ca^{2+} level was evaluated in this study. According to the report of Jiao *et al.*, oxidative stress reduces intracellular Ca^{2+} , which in turn leads to polyspermy by affecting cortical granule redistribution and causing the disorder of activation and damage to the microfilament network during the fertilization process [50]. Intracellular Ca^{2+} regulates a major event of mammalian cells and also regulates the cell cycle. In *Xenopus* eggs, CaMKII regulates the conversion of metaphase into anaphase in the meiotic cell cycle, and targeting Ca^{2+} /CaM and CaMKII stimulates the escape from metaphase arrest twice as much as continuous InsP3-dependent Ca^{2+} oscillations from MII to interphase in mouse oocytes [51]. Hence, we evaluated the intracellular Ca^{2+} level at the different nuclear stages during porcine IVM. In the non-treated groups, the intracellular Ca^{2+} level of GVBD- and MI-stage oocytes were higher than that of GV- and MII-stage cells. These results are consistent with previous reports that intracellular Ca^{2+} regulates the cell cycle [52–54]. Indeed, most matured oocytes arrested at the MII stage, and their intracellular Ca^{2+} levels were very low. In contrast, in the GT1b-treated groups, the intracellular Ca^{2+} levels at 40 hours were similar to those of the 18 hour maturation groups. These results indicated that GT1b could regulate intracellular Ca^{2+} during oocyte maturation, regardless of the cell cycle stage. Based on these results, the reason for ROS reduction without an increase in GSH might be the maintenance of intracellular Ca^{2+} levels by GT1b treatment.

Recently, it was confirmed that GT1b stimulates B2R signals in yeast cells that express mammalian B2R [55]. However, other studies using nonneuronal cells that also express B2R did not obtain a similar result [56]. An aim of the present study was to confirm whether B2R is expressed in matured porcine cumulus cells and oocytes. The expression of *B2R* was observed in cumulus cells but not in oocytes. *B2R* expression did not significantly differ from the zygote to blastocyst stage at different concentrations of GT1b treatment in the process of IVC in embryos that had been subjected to PA after the general IVM process (data not shown). Indeed, porcine PA/IVF was performed after the removal of cumulus cells, and zygotes produced from *in vitro* fertilization were cultured to

the blastocyst stage without cumulus cells. According to a previous hypothesis [32], GT1b is thought to directly affect cumulus cells and then increase intracellular Ca^{2+} in oocytes.

GT1b is distributed throughout in the granular layers [57], and it activates CaMKII distributed in synapses by activating *cdc42* [32]. CaMKII belongs to the serine/threonine protein kinase family and has 28 isoforms originating from alpha (α), beta (β), gamma (γ), and delta (δ) genes [58, 59]. It has been reported that CaMKII can interact with molecules that control Ca^{2+} signaling and the cell cycle in mouse oocytes [60]. In porcine oocytes, CaMKII is diversely involved in meiotic resumption and activation-like regulation of other proteins [61]. In a recent study using mouse oocytes, *CaMKII α* was found to be neuron specific, and *CaMKII β* was found primarily on neurons; neither of these isoforms are expressed in mouse oocytes [62, 63]. However, *CaMKII γ* and *CaMKII δ* are reportedly expressed in various tissues [63]. In this study, the expression of *CaMKII γ* and *CaMKII δ* was confirmed in porcine cumulus cells and oocytes. Backs *et al.* reported that oocytes from *CaMKII γ* -knockout mice could not exit metaphase II arrest in a meiotic resumption experiment [64]. However, the expression of exogenous *CaMKII γ* cDNA in the oocytes resulted in the resumption of meiosis, and this rescue might be possible with the expression of *CaMKII δ* because it is not isoform specific. Similar to this finding, *CaMKII γ* signaling is required to activate oocytes *in vivo*, downstream of Ca^{2+} oscillations [64]. Another previous study revealed that Ca^{2+} influx is required to activate downstream signaling molecules, including *CaMKII γ* , during meiotic resumption induced by sperm and during embryonic development. In particular, it was reported that *CaMKII γ* signaling is crucial in spindle rotation and polar body emission [65].

To understand the effect of GT1b in this study, oocytes were treated with different concentrations of GT1b during the process of IVM, and real-time PCR was carried out using cDNA obtained porcine cumulus cells and oocytes that had completed maturation. A previous study reported that B2R activates the PLC/PKC and cAMP/PKA pathways, and cAMP is known to inhibit cell growth [66]. Another study reported that cAMP/PKA pathway activation suppresses B2R and leads to the reduction of bradykinin-dependent inositol triphosphate and Ca^{2+} mobilization [67–69]. In the present study, the expression of *B2R* and *CaMKII δ* in cumulus cells from the 20 nM GT1b treatment group was significantly decreased compared with the control. This result showed that the expression of *B2R* is suppressed by cAMP/PKA pathway stimulation with GT1b treatment. Reduced *B2R* expression can lead to the suppression of another pathway of *B2R*, that is, the PLC/PKC pathway. As a result, it is thought that inositol triphosphate and Ca^{2+} mobilization are reduced and that the expression of *MAPK* is also decreased.

PCNA is known to be a critical gene in many cellular processes, such as DNA replication, DNA repair, DNA damage avoidance, cell cycle control, and cell survival. Recently, *PCNA* was reported to have an impact on the development of ovarian follicles [70–73]. However, the concentration of Ca^{2+} in oocytes was increased in the present study, and this would have stimulated the cell cycle and increased the expression of *POU5F1*. Furthermore, the expression of *CaMKII γ* and *CaMKII δ* tended to increase compared with the control, but the difference was not significant. It could be concluded that there was no significant effect on oocyte maturation because the concentration of

GT1b was not insufficient. In the 5 nM GT1b group, the expression of B2R in cumulus cells was slightly inhibited, but this inhibition was not significant. Like the other groups, the expression of *CaMKII δ* was decreased. Moreover, the Ca^{2+} concentration was increased in oocytes, and the expression of *CaMKII γ* was significantly increased. In a previous study, increased Ca^{2+} concentrations in mouse oocytes stimulated the activation of *CaMKII γ* , which led to the reduced activity of *MAPK* [65]. In addition, it was observed that *POU5F1* phosphorylation in human ES cells was dependent on *MAPK* [74], and *POU5F1* is thought to be downstream of *MAPK*, as shown in a recent study [75]. Therefore, it can be concluded that the increased expression of *CaMKII γ* decreases *MAPK* expression, which decreases *POU5F1* expression in oocytes. The additional NH_4^+ contained in the GT1b used in this experiment was previously reported to be cytotoxic [76]. Thus, we examined the expression of *Caspase-3*, but there were no significant differences.

Then PA and IVF were also carried out using GT1b-treated matured oocytes, but there were no significant differences among the treatment groups with regard to the cleavage rate, blastocyst formation rate, and the cell number in the blastocysts. However, embryo development rates showed a tendency to increase in a dose-dependent manner, but this trend was not significant. Therefore, treatment with a sufficient concentration of GT1b is thought to result in good quality oocytes.

The present study suggests that GT1b stimulates nuclear maturation at some concentrations, reduces ROS during IVM and inhibits cytoplasmic maturation by maintaining consistent intracellular Ca^{2+} levels regardless of the cell cycle. However, low concentrations of intracellular Ca^{2+} due to ROS or an inappropriate composition of the *in vitro* culture medium could be compensated for treatment with GT1b to raise the intracellular Ca^{2+} level to within the range comparable to that *in vivo*. Increased intracellular Ca^{2+} levels in the oocytes stimulated the cell cycle so that *POU5F1* expression also increased. It was reported in a previous study that the injection of 0.1 M CaCl_2 in metaphase II-arrested porcine oocytes readily activated cells [77]. Treatment with excessive levels of GT1b might activate matured oocytes. GT1b is thought to regulate the level of Ca^{2+} in oocytes in a dose-dependent manner and to be associated with another mechanism that controls the level of intracellular Ca^{2+} . Further studies are needed to confirm the changed level of intracellular Ca^{2+} in cumulus cells, and it is also necessary to determine the precise mechanism that maintains the intracellular Ca^{2+} level in oocytes.

Acknowledgments

This work was supported, in part, by a grant from the National Research Foundation of Korea Grant funded by the Korean Government (NRF-2013R1A2A2A04008751), Republic of Korea.

References

- Nagai T, Funahashi H, Yoshioka K, Kikuchi K. Up date of *in vitro* production of porcine embryos. *Front Biosci* 2006; **11**: 2565–2573. [Medline] [CrossRef]
- Laurent A, Pelage J-P, Wassef M, Martal J. Fertility after bilateral uterine artery embolization in a sheep model. *Fertil Steril* 2008; **89**(Suppl): 1371–1383. [Medline] [CrossRef]
- Chavatte-Palmer P, Al Gubory K, Picone O, Heyman Y. Maternal nutrition: effects on offspring fertility and importance of the periconceptual period on long-term development. *Gynecol Obstet Fertil* 2008; **36**: 920–929 (in French). [Medline] [CrossRef]
- Farahavar A, Shahne AZ. Effect of melatonin on *in vitro* maturation of bovine oocytes. *Afr J Biotechnol* 2010; **9**: 2579–2583.
- Casao A, Abecia J, Cebrián Pérez J, Muiño Blanco T, Vázquez M, Forcada F. The effects of melatonin on *in vitro* oocyte competence and embryo development in sheep. *Span J Agric Res* 2010; **8**: 35–41. [CrossRef]
- Choi J, Park SM, Lee E, Kim JH, Jeong YI, Lee JY, Park SW, Kim HS, Hossein MS, Jeong YW, Kim S, Hyun SH, Hwang WS. Anti-apoptotic effect of melatonin on preimplantation development of porcine parthenogenetic embryos. *Mol Reprod Dev* 2008; **75**: 1127–1135. [Medline] [CrossRef]
- Kwak S-S, Cheong S-A, Jeon Y, Lee E, Choi K-C, Jeung E-B, Hyun S-H. The effects of resveratrol on porcine oocyte *in vitro* maturation and subsequent embryonic development after parthenogenetic activation and *in vitro* fertilization. *Theriogenology* 2012; **78**: 86–101. [Medline] [CrossRef]
- Mukherjee A, Malik H, Saha AP, Dubey A, Singhal DK, Boateng S, Saugandhika S, Kumar S, De S, Guha SK, Malakar D. Resveratrol treatment during goat oocytes maturation enhances developmental competence of parthenogenetic and hand-made cloned blastocysts by modulating intracellular glutathione level and embryonic gene expression. *J Assist Reprod Genet* 2014; **31**: 229–239. [Medline] [CrossRef]
- Wang F, Tian X, Zhang L, He C, Ji P, Li Y, Tan D, Liu G. Beneficial effect of resveratrol on bovine oocyte maturation and subsequent embryonic development after *in vitro* fertilization. *Fertil Steril* 2014; **101**: 577–586. [Medline] [CrossRef]
- Reed ML, Estrada JL, Illera MJ, Petters RM. Effects of epidermal growth factor, insulin-like growth factor-I, and dialyzed porcine follicular fluid on porcine oocyte maturation *in vitro*. *J Exp Zool* 1993; **266**: 74–78. [Medline] [CrossRef]
- Loneragan P, Carolan C, Van Langendonck A, Donnay I, Khatir H, Mermillod P. Role of epidermal growth factor in bovine oocyte maturation and preimplantation embryo development *in vitro*. *Biol Reprod* 1996; **54**: 1420–1429. [Medline] [CrossRef]
- Lighten AD, Hardy K, Winston RM, Moore GE. Expression of mRNA for the insulin-like growth factors and their receptors in human preimplantation embryos. *Mol Reprod Dev* 1997; **47**: 134–139. [Medline] [CrossRef]
- Kwak SS, Jeung SH, Biswas D, Jeon YB, Hyun SH. Effects of porcine granulocyte-macrophage colony-stimulating factor on porcine *in vitro*-fertilized embryos. *Theriogenology* 2012; **77**: 1186–1197. [Medline] [CrossRef]
- Einspanier R, Schönfelder M, Müller K, Stojkovic M, Kosmann M, Wolf E, Schams D. Expression of the vascular endothelial growth factor and its receptors and effects of VEGF during *in vitro* maturation of bovine cumulus-oocyte complexes (COC). *Mol Reprod Dev* 2002; **62**: 29–36. [Medline] [CrossRef]
- Biswas D, Jung EM, Jeung EB, Hyun SH. Effects of vascular endothelial growth factor on porcine preimplantation embryos produced by *in vitro* fertilization and somatic cell nuclear transfer. *Theriogenology* 2011; **75**: 256–267. [Medline] [CrossRef]
- Kwak DH, Seo BB, Chang KT, Choo YK. Roles of gangliosides in mouse embryogenesis and embryonic stem cell differentiation. *Exp Mol Med* 2011; **43**: 379–388. [Medline] [CrossRef]
- Huwiler A, Kolter T, Pfeilschifter J, Sandhoff K. Physiology and pathophysiology of sphingolipid metabolism and signaling. *Biochim Biophys Acta* 2000; **1485**: 63–99. [Medline] [CrossRef]
- Svennerholm L, Fredman P. A procedure for the quantitative isolation of brain gangliosides. *Biochim Biophys Acta* 1980; **617**: 97–109. [Medline] [CrossRef]
- Yu RK, Bieberich E, Xia T, Zeng G. Regulation of ganglioside biosynthesis in the nervous system. *J Lipid Res* 2004; **45**: 783–793. [Medline] [CrossRef]
- Nakamura K, Inagaki F, Tamai Y. A novel ganglioside in dogfish brain. Occurrence of a trisialoganglioside with a sialic acid linked to N-acetylgalactosamine. *J Biol Chem* 1988; **263**: 9896–9900. [Medline]
- Yu RK, Tsai Y-T, Ariga T, Yanagisawa M. Structures, biosynthesis, and functions of gangliosides—an overview. *J Oleo Sci* 2011; **60**: 537–544. [Medline] [CrossRef]
- Yamamoto HA, Mohanan PV. Ganglioside GT1B and melatonin inhibit brain mitochondrial DNA damage and seizures induced by kainic acid in mice. *Brain Res* 2003; **964**: 100–106. [Medline] [CrossRef]
- Gavella M, Garaj-Vrhovac V, Lipovac V, Antica M, Gajski G, Car N. Ganglioside GT1b protects human spermatozoa from hydrogen peroxide-induced DNA and membrane damage. *Int J Androl* 2010; **33**: 536–544. [Medline] [CrossRef]
- Gavella M, Lipovac V. Protective effects of exogenous gangliosides on ROS-induced changes in human spermatozoa. *Asian J Androl* 2013; **15**: 375–381. [Medline] [CrossRef]
- Kim B-H, Jung J-U, Ko K, Kim W-S, Kim S-M, Ryu J-S, Jin J-W, Yang H-J, Kim J-S, Kwon H-C, Nam SY, Kwak DH, Park YI, Koo DB, Choo YK. Expression of ganglioside GT1b in mouse embryos at different developmental stages after cryopreservation. *Arch Pharm Res* 2008; **31**: 88–95. [Medline] [CrossRef]
- Chen N, Furuya S, Doi H, Hashimoto Y, Kudo Y, Higashi H. Ganglioside/calmodulin kinase II signal inducing cdc42-mediated neuronal actin reorganization. *Neuroscience* 2003; **120**: 163–176. [Medline] [CrossRef]
- Yanaga F, Hirata M, Koga T. Evidence for coupling of bradykinin receptors to a guanine-nucleotide binding protein to stimulate arachidonate liberation in the osteoblast-like cell

- line, MC3T3-E1. *Biochim Biophys Acta* 1991; **1094**: 139–146. [Medline] [CrossRef]
28. **Chen H, Kui C, Chan HC.** Ca²⁺ mobilization in cumulus cells: role in oocyte maturation and acrosome reaction. *Cell Calcium* 2013; **53**: 68–75. [Medline] [CrossRef]
 29. **You J, Kim J, Lim J, Lee E.** Anthocyanin stimulates *in vitro* development of cloned pig embryos by increasing the intracellular glutathione level and inhibiting reactive oxygen species. *Theriogenology* 2010; **74**: 777–785. [Medline] [CrossRef]
 30. **Nasr-Esfahani MH, Aitken JR, Johnson MH.** Hydrogen peroxide levels in mouse oocytes and early cleavage stage embryos developed *in vitro* or *in vivo*. *Development* 1990; **109**: 501–507. [Medline]
 31. **Livak KJ, Schmittgen TD.** Analysis of relative gene expression data using real-time quantitative PCR and the 2(-ΔΔC(T)) Method. *Methods* 2001; **25**: 402–408. [Medline] [CrossRef]
 32. **Kotani M, Kawashima I, Ozawa H, Ogura K, Ishizuka I, Terashima T, Tai T.** Immunohistochemical localization of minor gangliosides in the rat central nervous system. *Glycobiology* 1994; **4**: 855–865. [Medline] [CrossRef]
 33. **Kwak S-S, Yoon JD, Cheong S-A, Jeon Y, Lee E, Hyun S-H.** The new system of shorter porcine oocyte *in vitro* maturation (18 hours) using ≥8 mm follicles derived from cumulus-oocyte complexes. *Theriogenology* 2014; **81**: 291–301. [Medline] [CrossRef]
 34. **Yamamoto HA, Mohanan PV.** *In vivo* and *in vitro* effects of melatonin or ganglioside GT1B on L-cysteine-induced brain mitochondrial DNA damage in mice. *Toxicol Sci* 2003; **73**: 416–422. [Medline] [CrossRef]
 35. **Sonnino S, Cantù L, Corti M, Acquotti D, Venerando B.** Aggregative properties of gangliosides in solution. *Chem Phys Lipids* 1994; **71**: 21–45. [Medline] [CrossRef]
 36. **Gavella M, Kveder M, Lipovac V.** Modulation of ROS production in human leukocytes by ganglioside micelles. *Braz J Med Biol Res* 2010; **43**: 942–949. [Medline] [CrossRef]
 37. **de Matos DG, Furnus CC.** The importance of having high glutathione (GSH) level after bovine *in vitro* maturation on embryo development effect of β-mercaptoethanol, cysteine and cystine. *Theriogenology* 2000; **53**: 761–771. [Medline] [CrossRef]
 38. **Sanocka D, Miesel R, Jedrzejczak P, Kurpius MK.** Oxidative stress and male infertility. *J Androl* 1996; **17**: 449–454. [Medline]
 39. **Aitken RJ, Roman SD.** Antioxidant systems and oxidative stress in the testes. *Oxid Med Cell Longev* 2008; **1**: 15–24. [Medline] [CrossRef]
 40. **Lin C-M, Chen C-T, Lee H-H, Lin J-K.** Prevention of cellular ROS damage by isovitamin and related flavonoids. *Planta Med* 2002; **68**: 365–367. [Medline] [CrossRef]
 41. **Cabiscol E, Tamarit J, Ros J.** Oxidative stress in bacteria and protein damage by reactive oxygen species. *Int Microbiol* 2000; **3**: 3–8. [Medline]
 42. **Gardner PR, Fridovich I.** Superoxide sensitivity of the Escherichia coli 6-phosphogluconate dehydratase. *J Biol Chem* 1991; **266**: 1478–1483. [Medline]
 43. **Imlay JA, Linn S.** DNA damage and oxygen radical toxicity. *Science* 1988; **240**: 1302–1309. [Medline] [CrossRef]
 44. **Harris ED.** Regulation of antioxidant enzymes. *FASEB J* 1992; **6**: 2675–2683. [Medline]
 45. **Hussain S, Slikker W Jr, Ali SF.** Age-related changes in antioxidant enzymes, superoxide dismutase, catalase, glutathione peroxidase and glutathione in different regions of mouse brain. *Int J Dev Neurosci* 1995; **13**: 811–817. [Medline] [CrossRef]
 46. **Goto Y, Noda Y, Mori T, Nakano M.** Increased generation of reactive oxygen species in embryos cultured *in vitro*. *Free Radic Biol Med* 1993; **15**: 69–75. [Medline] [CrossRef]
 47. **Johnson MH, Nasr-Esfahani MH.** Radical solutions and cultural problems: could free oxygen radicals be responsible for the impaired development of preimplantation mammalian embryos *in vitro*? *BioEssays* 1994; **16**: 31–38. [Medline] [CrossRef]
 48. **Luvoni GC, Keskinetepe L, Brackett BG.** Improvement in bovine embryo production *in vitro* by glutathione-containing culture media. *Mol Reprod Dev* 1996; **43**: 437–443. [Medline] [CrossRef]
 49. **Halliwell B, Gutteridge JM.** Free radicals and antioxidant protection: mechanisms and significance in toxicology and disease. *Hum Toxicol* 1988; **7**: 7–13. [Medline] [CrossRef]
 50. **Jiao G-Z, Cao X-Y, Cui W, Lian H-Y, Miao Y-L, Wu X-F, Han D, Tan J-H.** Developmental potential of prepubertal mouse oocytes is compromised due mainly to their impaired synthesis of glutathione. *PLoS ONE* 2013; **8**: e58018. [Medline] [CrossRef]
 51. **Kahl CR, Means AR.** Regulation of cell cycle progression by calcium/calmodulin-dependent pathways. *Endocr Rev* 2003; **24**: 719–736. [Medline] [CrossRef]
 52. **Ciapa B, Pesando D, Wilding M, Whitaker M.** Cell-cycle calcium transients driven by cyclic changes in inositol trisphosphate levels. *Nature* 1994; **368**: 875–878. [Medline] [CrossRef]
 53. **Whitaker M, Patel R.** Calcium and cell cycle control. *Development* 1990; **108**: 525–542. [Medline]
 54. **Clapham DE.** Calcium signaling. *Cell* 1995; **80**: 259–268. [Medline] [CrossRef]
 55. **Kanatsu Y, Chen NH, Mitoma J, Nakagawa T, Hirabayashi Y, Higashi H.** Gangliosides stimulate bradykinin B2 receptors to promote calmodulin kinase II-mediated neuronal differentiation. *J Biochem* 2012; **152**: 63–72. [Medline] [CrossRef]
 56. **Shimazaki A, Nakagawa T, Mitoma J, Higashi H.** Gangliosides and chondroitin sulfate desensitize and internalize B2 bradykinin receptors. *Biochem Biophys Res Commun* 2012; **420**: 193–198. [Medline] [CrossRef]
 57. **Kotani M, Kawashima I, Ozawa H, Terashima T, Tai T.** Differential distribution of major gangliosides in rat central nervous system detected by specific monoclonal antibodies. *Glycobiology* 1993; **3**: 137–146. [Medline] [CrossRef]
 58. **Baltas LG, Karczewski P, Krause EG.** The cardiac sarcoplasmic reticulum phospholamban kinase is a distinct δ-CaM kinase isozyme. *FEBS Lett* 1995; **373**: 71–75. [Medline] [CrossRef]
 59. **Hudmon A, Schulman H.** Neuronal CA2+/calmodulin-dependent protein kinase II: the role of structure and autoregulation in cellular function. *Annu Rev Biochem* 2002; **71**: 473–510. [Medline] [CrossRef]
 60. **Su YQ, Eppig JJ.** Evidence that multifunctional calcium/calmodulin-dependent protein kinase II (CaM KII) participates in the meiotic maturation of mouse oocytes. *Mol Reprod Dev* 2002; **61**: 560–569. [Medline] [CrossRef]
 61. **Fan H-Y, Huo L-J, Meng X-Q, Zhong Z-S, Hou Y, Chen D-Y, Sun Q-Y.** Involvement of calcium/calmodulin-dependent protein kinase II (CaMKII) in meiotic maturation and activation of pig oocytes. *Biol Reprod* 2003; **69**: 1552–1564. [Medline] [CrossRef]
 62. **Takaishi T, Saito N, Tanaka C.** Evidence for distinct neuronal localization of γ and δ subunits of Ca2+/calmodulin-dependent protein kinase II in the rat brain. *J Neurochem* 1992; **58**: 1971–1974. [Medline] [CrossRef]
 63. **Bayer KU, Löhler J, Schulman H, Harbers K.** Developmental expression of the CaM kinase II isoforms: ubiquitous γ- and δ-CaM kinase II are the early isoforms and most abundant in the developing nervous system. *Brain Res Mol Brain Res* 1999; **70**: 147–154. [Medline] [CrossRef]
 64. **Backs J, Stein P, Backs T, Duncan FE, Grueter CE, McAnally J, Qi X, Schultz RM, Olson EN.** The γ isoform of CaM kinase II controls mouse egg activation by regulating cell cycle resumption. *Proc Natl Acad Sci USA* 2010; **107**: 81–86. [Medline] [CrossRef]
 65. **Miao Y-L, Stein P, Jefferson WN, Padilla-Banks E, Williams CJ.** Calcium influx-mediated signaling is required for complete mouse egg activation. *Proc Natl Acad Sci USA* 2012; **109**: 4169–4174. [Medline] [CrossRef]
 66. **Iwashita S, Mitsui K, Shoji-Kasai Y, Senshu-Miyaike M.** cAMP-mediated modulation of signal transduction of epidermal growth factor (EGF) receptor systems in human epidermoid carcinoma A431 cells. Depression of EGF-dependent diacylglycerol production and EGF receptor phosphorylation. *J Biol Chem* 1990; **265**: 10702–10708. [Medline]
 67. **Campbell MD, Subramaniam S, Kotlikoff MI, Williamson JR, Fluharty SJ.** Cyclic AMP inhibits inositol polyphosphate production and calcium mobilization in neuroblastoma X glioma NG108-15 cells. *Mol Pharmacol* 1990; **38**: 282–288. [Medline]
 68. **Luo SF, Chiu CT, Tsao HL, Fan LW, Tsai CT, Pan SL, Yang CM.** Effect of forskolin on bradykinin-induced calcium mobilization in cultured canine tracheal smooth muscle cells. *Cell Signal* 1997; **9**: 159–167. [Medline] [CrossRef]
 69. **Mizumura K, Sugiura T, Katanosaka K, Banik RK, Kozaki Y.** Excitation and sensitization of nociceptors by bradykinin: what do we know? *Exp Brain Res* 2009; **196**: 53–65. [Medline] [CrossRef]
 70. **Langerak P, Nygren AO, Krijger PH, van den Berk PC, Jacobs H.** A/T mutagenesis in hypermutated immunoglobulin genes strongly depends on PCNAK164 modification. *J Exp Med* 2007; **204**: 1989–1998. [Medline] [CrossRef]
 71. **Prakash S, Johnson RE, Prakash L.** Eukaryotic translesion synthesis DNA polymerases: specificity of structure and function. *Annu Rev Biochem* 2005; **74**: 317–353. [Medline] [CrossRef]
 72. **Helleday T, Lo J, van Gent DC, Engelward BP.** DNA double-strand break repair: from mechanistic understanding to cancer treatment. *DNA Repair (Amst)* 2007; **6**: 923–935. [Medline] [CrossRef]
 73. **Stoimenov I, Helleday T.** PCNA on the crossroad of cancer. *Biochem Soc Trans* 2009; **37**: 605–613. [Medline] [CrossRef]
 74. **Brumbaugh J, Hou Z, Russell JD, Howden SE, Yu P, Ledvina AR, Coon JJ, Thomson JA.** Phosphorylation regulates human OCT4. *Proc Natl Acad Sci USA* 2012; **109**: 7162–7168. [Medline] [CrossRef]
 75. **Frum T, Halbisen MA, Wang C, Amiri H, Robson P, Ralston A.** Oct4 cell-autonomously promotes primitive endoderm development in the mouse blastocyst. *Dev Cell* 2013; **25**: 610–622. [Medline] [CrossRef]
 76. **Martinelle K, Haggström L.** Mechanisms of ammonia and ammonium ion toxicity in animal cells: transport across cell membranes. *J Biotechnol* 1993; **30**: 339–350. [Medline] [CrossRef]
 77. **Macháty Z, Funahashi H, Mayes MA, Day BN, Prather RS.** Effects of injecting calcium chloride into *in vitro*-matured porcine oocytes. *Biol Reprod* 1996; **54**: 316–322. [Medline] [CrossRef]